

Use of the hydrodistillation residue of the essential oil of pink pepper (*Schinus terebinthifolius* Raddi) in the corrosion protection of carbon steel in HCl medium

Utilização do resíduo da hidrodestilação do óleo essencial de pimenta rosa (*Schinus terebinthifolius* Raddi) na proteção contra corrosão de aço carbono em meio HCl

Uso del residuo de hidrodestilación del aceite esencial de pimienta rosa (*Schinus terebinthifolius* Raddi) en la protección contra la corrosión del acero al carbono en medio HCl

Received: 09/26/2022 | Revised: 10/03/2022 | Accepted: 10/05/2022 | Published: 10/11/2022

Nayara Maria Santos de Almeida

ORCID: <https://orcid.org/0000-0003-1933-6092>

Universidade Estadual de Santa Cruz, Brazil

E-mail: nayaraalmeida226@gmail.com

Iago Magella Fernandes Costa Rossi e Silva

ORCID: <https://orcid.org/0000-0003-4639-2540>

Universidade Estadual de Santa Cruz, Brazil

E-mail: iago.magella6@gmail.com

Brunela Pereira da Silva

ORCID: <https://orcid.org/0000-0003-2560-6968>

Universidade de São Paulo, Brazil

E-mail: brunelapereira@usp.br

Fernando Cotting

ORCID: <https://orcid.org/0000-0001-5980-0078>

Universidade Federal de Minas Gerais, Brazil

E-mail: fernandocotting@gmail.com

Idalina Vieira Aoki

ORCID: <https://orcid.org/0000-0002-8203-2625>

Universidade de São Paulo, Brazil

E-mail: idavaoki@usp.br

Tácia Costa Veloso

ORCID: <https://orcid.org/0000-0003-0444-7304>

Universidade Federal do Sul da Bahia, Brazil

E-mail: taciaveloso@yahoo.com.br

Vera Rosa Capelossi

ORCID: <https://orcid.org/0000-0002-0212-8388>

Universidade Estadual de Santa Cruz, Brazil

E-mail: vrcafelossi@uesc.br

Abstract

In this research, different concentrations of the powder of the solid residue from the hydrodistillation of the pink pepper leaf (PRHPPL), generated in the production of its essential oil, were evaluated as an inhibitor for carbon steel in HCl 0.5 mol L⁻¹. This evaluation was performed using electrochemical impedance spectroscopy (EIS), potentiodynamic polarization, scanning vibrating electrode technique (SVET), and mass loss tests. All tests showed that the highest concentration of the inhibitor (1.77 g L⁻¹) presented better efficiency; from i_{corr} , this efficiency was 98 %, from the equivalent circuit model R_{ct} value it was 98 % and by the gravimetric test it was 86 %. Different isotherms were tested in order to better understand the adsorption process of the inhibitor molecules on the metal surface and the best fit was found for the Langmuir isotherm. The morphology of the steel surface was also analyzed by scanning electron microscopy (SEM). This study reveals that this residue obtained from the production of essential oils can be used as corrosion inhibitor in the replacement to synthetic inhibitors.

Keywords: Corrosion; Natural inhibitor; Pink pepper; SVET; Adsorption isotherms.

Resumo

Nessa pesquisa, foram avaliadas diferentes concentrações do pó do resíduo sólido da hidrodestilação da folha de pimenta rosa (PRHPPL), gerado na produção de seu óleo essencial, como inibidor para aço carbono em HCl 0,5 mol L⁻¹. Esta avaliação foi realizada por meio de espectroscopia de impedância eletroquímica (EIS), polarização potenciodinâmica, técnica de varredura de eletrodo vibratório (SVET) e testes de perda de massa. Todos os testes

mostraram que a maior concentração do inibidor ($1,77 \text{ g L}^{-1}$) apresentou melhor eficiência; do icorr, essa eficiência foi de 98%, do modelo de circuito equivalente R_{ct} valor foi de 98% e pelo teste gravimétrico foi de 86%. Diferentes isotermas foram testadas a fim de entender melhor o processo de adsorção das moléculas inibidoras na superfície do metal e o melhor ajuste foi encontrado para a isoterma de Langmuir. A morfologia da superfície do aço também foi analisada por microscopia eletrônica de varredura (MEV). Este estudo revela que este resíduo obtido da produção de óleos essenciais pode ser utilizado como inibidor de corrosão em substituição aos inibidores sintéticos.

Palavras-chave: Corrosão, Inibidor natural, Pimenta rosa, SVET, Isotérmicas de adsorção.

Resumen

En esta investigación, se evaluaron diferentes concentraciones del polvo del residuo sólido de la hidrodestilación de la hoja de ají rosa (PRHPPL), generado en la producción de su aceite esencial, como inhibidor del acero al carbono en $\text{HCl } 0.5 \text{ mol L}^{-1}$. Esta evaluación se realizó mediante espectroscopia de impedancia electroquímica (EIS), polarización potenciodinámica, técnica de exploración de electrodos vibratorios (SVET) y pruebas de pérdida de masa. Todas las pruebas mostraron que la mayor concentración del inhibidor (1.77 g L^{-1}) presentó mejor eficiencia; de icorr, esta eficiencia fue del 98 %, del modelo de circuito equivalente valor R_{ct} fue del 98 % y por la prueba gravimétrica fue del 86 %. Se probaron diferentes isotermas para comprender mejor el proceso de adsorción de las moléculas inhibidoras en la superficie del metal y se encontró el mejor ajuste para la isoterma de Langmuir. La morfología de la superficie del acero también se analizó mediante microscopía electrónica de barrido (SEM). Este estudio revela que este residuo obtenido de la producción de aceites esenciales puede ser utilizado como inhibidor de corrosión en reemplazo de inhibidores sintéticos.

Palabras clave: Corrosión; Inhibidor natural; Pimienta rosa; SVET; Isotermas de adsorción.

1. Introduction

Carbon steel is widely used in various industrial sectors and also civil society. Monuments, bridges, pipes, automobile parts and hospital equipment are just a few examples where this material is applied. This steel's versatility is due to the characteristics such as good weldability, good mechanical resistance and low cost. Despite these advantages, carbon steel has the inconvenience of low corrosion resistance, thus requiring a protection mechanism, in order to not affect the benefits of using this alloy (Anupama *et al.*, 2017).

Atmospheres with acidic pH and containing chloride ions (Cl^-), bromides (Br^-) and iodides (I^-) promote an accentuated corrosion of carbon steel. Acid solutions are widely used in various industrial processes such as pickling, acidification of oil wells and others. An acid solution widely used in the industrial environment is of hydrochloric acid (HCl), and in some industrial processes, such as oil platform towers, this acid is produced. In the oil industry, the overhead system of the crude tower condenses the water, which absorbs the hydrogen chloride, creating hydrochloric acid. Hydrochloric acid solution in industrial processes creates potential corrosion or dissolution on surface deposits promoting corrosion of metals such as carbon steel (Speight, 2014).

Among the strategies aimed at controlling corrosion, the use of corrosion inhibitors is widely chosen due to their low cost and easy application, and can be applied in situ, without the need to interrupt industrial processes. These inhibitors are substances or combinations of them that, when inserted in the corrosive medium, slows down the destructive action of this medium on the material. For many years, synthetic chemical inhibitors, such as those from chromium, were used due to their good efficiency, however, the harmful effect on the environment and human beings, led to the search for efficient and non-toxic inhibitors, resulting in natural inhibitors of corrosion (Umoren *et al.*, 2019).

These green inhibitors come from different species and plant parts such as leaves (Al Hasan *et al.*, 2019; Ogunleye *et al.*, 2020), seeds (Zaher *et al.*, 2020), bark (Barreto *et al.*, 2017; Barreto *et al.*, 2018; Saeed *et al.*, 2020), oils (Loto *et al.*, 2018; Tolulope & Olowoyo, 2018), flower (Divya *et al.*, 2019), and fruit (Sanaei *et al.*, 2019). The inhibitory action of natural products is attributed to the presence of flavonoids, alkaloids, nitrogenous bases, carbohydrates and proteins that help in their anticorrosive action, in addition to the presence of heteroatoms together with functional groups (Umoren *et al.*, 2019) that favors the adsorption to the metal's surface.

A plant popularly called pink pepper, inside the *Schinus terebinthifolius* Raddi species, is widely known and used for many years for its numerous benefits, such as antimicrobial and antioxidant capacity. Pink pepper is among the aromatic plants used as raw material to essential oil industries, which extract the essential oil from its different parts. There are different extraction processes for these oils where hydrodistillation is being one of the most popular because of its simplicity. In this process, the plant material is placed in a container containing water and the distillation takes place at a temperature of around 100°C, depending on the location, as the boiling temperature of water depends on the pressure. For this process, as well as others used in the extraction of essential oils, there is a need for a large mass of the vegetable product to obtain a satisfactory amount of essential oil. This vegetable mass is discarded after the extraction process, but it may have potential for reuse, as a use in the protection against corrosion of materials such as carbon steel (Baranauskienė *et al.*, 2019; Elyemni *et al.*, 2019; Mahomoodally *et al.*, 2019; Santana *et al.*, 2012; Uliana *et al.*, 2016; Veličković *et al.*, 2008).

Therefore, this work aims to investigate the potential of the powder from the hydrodistillation residue of the essential oil of the pink pepper leaf as a corrosion inhibitor of ASTM 1008 carbon steel in 0.5 mol L⁻¹ HCl medium. This research can promote a new alternative for corrosion control, being an economically and environmentally viable alternative when compared to synthetic corrosion inhibitors. In addition, it can make the production of essential oils more sustainable because in this production there is an excessive use of vegetable mass that generates a waste discarded by this industry. The present study can be an effective means of using this residue.

2. Methodology

The present research is a study carried out in the laboratory. It has a qualitative and quantitative nature aiming at the analysis of a residue from the production of essential oil as a natural corrosion inhibitor of materials. The purpose of the work is to verify if this residue can be used as an inhibitor and if this question is true, what efficiency can this inhibitor achieve.

The methodology used is the standard used in the area of corrosion of materials. Some authors who studied some residues as a natural corrosion inhibitor used this same methodology, such as Santos *et al.* (2021) in their study on Palmiste pie powder as a natural corrosion inhibitor; and Carvalho *et al.* (2022) in their study of cocoa bean husk as a natural corrosion inhibitor. For a better understanding of the research, the experimental part is divided into preparation of the residue that will be tested as an inhibitor, preparation of the metal that will be used as a substrate, the characteristic tests of the corrosion area (electrochemical and gravimetric) and finally a characterization through Scanning Electron Microscopy and Energy Dispersive X-Ray Spectroscopy. You can see this methodology in more detail below.

2.1 Inhibitor Preparation

The natural product used as a natural inhibitor was the leaf of the pink pepper plant of the *Schinus terebinthifolius* Raddi species. The leaves were collected in Ilhéus, state of Bahia. These leaves underwent a hydrodistillation process in a cleverger device, after extracting the essential oil, the leaf was removed from the device and filtered to remove excess water from the process. Then the leaves were dried in an oven at 40°C for 4 hours and crushed in a knife mill. The product resulting from this grinding was then sieved through a Tyler sieve system and the powder with a granulometry less than 170 mesh was used as an inhibitor. This inhibitor, derived from the powder of the residue of the hydrodistillation of the pink pepper leaf (PRHPPL), was added to the electrolyte (HCl 0.5 mol.L⁻¹) at different concentrations (0.44 g L⁻¹, 0.77 g L⁻¹, 1.11 g L⁻¹, 1.44 g L⁻¹ and 1.77 g L⁻¹), following the studies of Santos *et al.* (Santos *et al.*, 2017).

2.2 Preparation of carbon steel surface

The carbon steel samples were previously cut in the dimensions of 20 x 20 x 8 mm and then cleaned with water and ethanol. After this cleaning, the steel plate was placed for 10 minutes in an ultrasonic bath with acetone; after sonication, the samples were washed with distilled water and immersed in degreaser (Saloclean solution) for 10 minutes at 60 °C. After the degreasing, the samples were washed with distilled water and then dried. Finally, an acid pickling was performed for 30 seconds, in a 3.0 mol L⁻¹ HCl solution, to remove possible corrosion pre-products, and then washed with distilled water and dried.

2.3 Electrochemical Tests

Electrochemical tests were performed in triplicate, in the presence and absence of the corrosion inhibitor. The inhibition efficiency results come from the average of the values obtained from the triplicate and the corresponding standard deviation. The tests were carried out in an electrochemical cell with three electrodes, the reference electrode being Ag|AgCl|KCl sat, the counter electrode a rhodium-coated titanium wire and the working electrode was the carbon steel sample. The electrolyte used was an aqueous solution of 0.5 molL⁻¹ HCl.

Initially, the open circuit potential was monitored until its stabilization. Then, the measurements of electrochemical impedance spectroscopy (EIS) was performed in the frequency range from 100 kHz to 10 mHz, with a disturbance amplitude of 10 mV (rms). Finally, the potentiodynamic polarization of the samples was performed, polarizing the electrodes in the range ± 250 mV vs OCP (open circuit potential), with a scan rate of 0.5 mV s⁻¹. From the Tafel curves obtained for each inhibitor concentration, the corrosion current density (i_{corr}) was determined. This density was obtained by drawing a straight line for the points of potential, subtracting or adding 50 mV in relation to OCP (using the OriginPro 2016 software) representative of the cathodic and anodic branch of the curve. For each straight line, its tangent or pendent was also drawn and the intersection of the anodic and cathodic tangents with E_{corr} horizontal line was considered the i_{corr} .

The SVET tests were performed using Applicable Electronics Inc. equipment, controlled by the ASET-Sciencewares auxiliary software. The microprobe used was a platinum/iridium vibrating probe with 10 μm diameter of platinum deposit at the tip of the probe. The measurements were carried out using a electrolyte solution of 0.01mol L⁻¹ HCl solution in the presence and absence of the inhibitor in the same concentration that showed the best efficiency by the EIS measurements. The exposed area of carbon steel was delimited with beeswax.

During the test, the distance used between the sample surface and the vibrating probe was 100 μm and the ionic current maps were acquired after 30, 60, 300 and 600 min of carbon steel immersion in the electrolyte.

2.4 Gravimetric Test

This assay was also performed in triplicate and the mean value was used for analysis. The carbon steel sample was immersed in a 0.5 mol L⁻¹ HCl solution in the absence and presence of different concentrations (0.44 g L⁻¹, 0.77 g L⁻¹, 1.11 g L⁻¹, 1.44 g L⁻¹ and 1.77 g L⁻¹) of the inhibitor (PRHFPR). The weight loss tests were performed according to ASTM G1-03 (Reapproved 2017) and the sample was immersed in the corrosive medium for 2h.

2.5 Scanning Electron Microscopy/Energy Dispersive X-ray Spectroscopy (SEM/EDS)

Morphological analysis by SEM was performed for samples after undergoing gravimetric testing without and with the presence of the inhibitor. A carbon steel control sample was also analyzed for comparison of the results. Also, the chemical elemental analysis was performed.

The MEV equipment used was from Tescan, model Vega 3 LMU coupled with an Oxford Instruments X-ray detector. The images were obtained by secondary electrons (SE), with the operating voltage of 20 kV. The cathode was a tungsten filament.

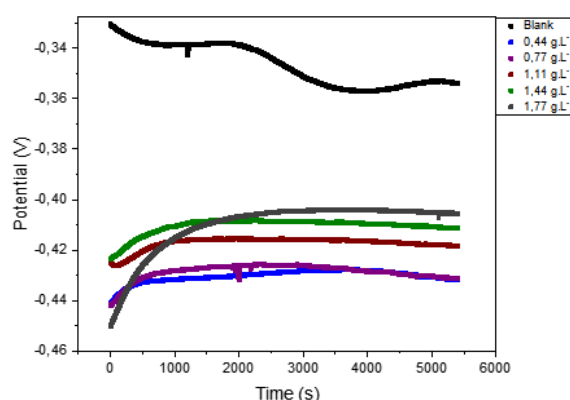
3. Results and Discussion

3.1 Electrochemical Tests

3.1.1 Open Circuit Potential (OCP)

The variation of the potential with time for carbon steel in a 0.5 mol L⁻¹ HCl solution in the absence and presence of different concentrations of PRHPPL can be seen in Figure 1. Stable OCP values were reached after approximately 4000 s, and the maximum time used for complete stabilization, for all conditions under analysis, was 5400 s. In the test in the absence of inhibitor, the OCP value decreases after 3000 s, due to the dissolution of the steel surface previous oxide layer, and stabilizes at the approximate value of -360 mV after 5400 s of immersion. The addition of the inhibitor at different concentrations in the electrolyte changed the behavior of the OCP, leading to an increase in the potential right at the beginning of the immersion. In all concentrations, the OCP was stabilized at more negative values, indicating that the inhibitor preferentially inhibits cathodic reactions.

Figure 1: OCP curves of carbon steel samples in HCl 0.5 molL⁻¹ in the absence and presence of different concentration of PRHPPL at room temperature.



Source: Authors.

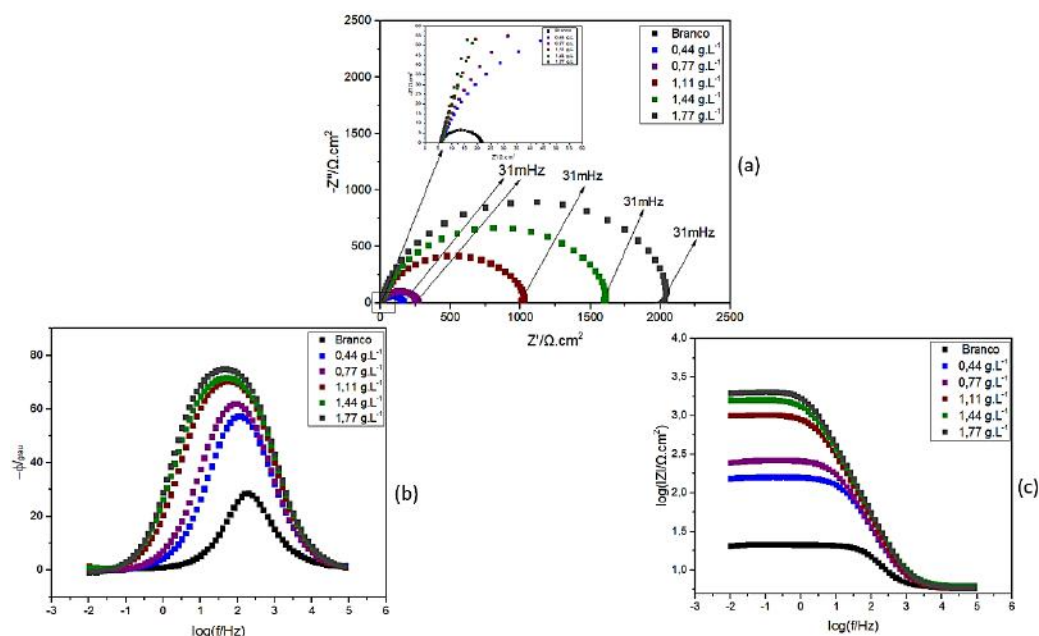
3.1.2 Electrochemical Impedance Spectroscopy (EIS)

Figure 2 shows the Nyquist (a) and Bode diagrams, phase angle (b) and logarithm of the impedance modulus (c), obtained in the absence and presence of different concentrations of PRHPPL. With these diagrams it is possible to evaluate the corrosion resistance of carbon steel SAE 1008 in a 0.5 mol L⁻¹ solution and the measurements were obtained after stabilization of the OCP.

In Nyquist diagrams (Figure, 2.a) it is observed a capacitive arc for the control sample which is connected to the electrochemical process of charge transfer at the interface of the metal/electrolyte. The shape of the arc does not change with the addition of the inhibitor, indicating that its presence does not change the electrochemical mechanism of the system (Santos *et al.*, 2020). Furthermore, it can be seen that increasing the concentration of the inhibitor promotes an increase in the diameter of the capacitive arc, reaching the highest value for the highest concentration (1.77 g L⁻¹) evaluated; thus, showing that for this concentration the greatest resistance to corrosion was achieved.

The Bode diagrams of phase angle (Figure 2.b) and logarithm of the impedance modulus (Figure 2.c) it is also verified that the increase in the inhibitor concentration led to a large increase in the phase angle values. For the condition without inhibitor, the maximum phase angle was 29° and for the highest concentration of inhibitor, the maximum phase angle was 76° . This large increase in the phase angle value, in almost the entire analyzed frequency range, is the result of the adsorption of a higher number of inhibitory substances on the metallic surface, increasing the degree of protection against corrosion. Looking at the Bode diagrams, it becomes clearer to note that there is a single time constant for all conditions studied. Therefore, the higher values of impedance modulus in the low frequency region, in the presence of inhibitor, reveal that there is an increase in the charge transfer resistance of these electrochemical systems, when compared to the control sample, without inhibitor (Ituen *et al.*, 2017).

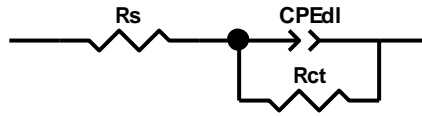
Figure 2: Nyquist diagram (a) and Bode diagrams phase angle (b) and logarithm of the impedance modulus (c) of carbon steel in the absence and presence of different concentrations of PRHPPL in 0.5 molL^{-1} HCl at room temperature.



Source: Authors.

The impedance diagrams (Figure 2) enable a qualitative analysis of the effect of adding PRHPPL inhibitor in the electrolyte on the steel surface, whether or not this addition promotes an increase in the corrosion resistance of carbon steel. As seen in the diagrams in Figure 2, the highest concentration of PRHPPL was the one that presented the greatest resistance, hence the greatest efficiency. To find out how efficient the inhibitor was in a more precise way, a quantitative analysis was performed by fitting the data obtained using an equivalent circuit. The circuit model used, a simple Randles circuit, was the one shown in Figure 3, a circuit traditionally used in studies of natural inhibitors (Barreto *et al.*, 2017; Barreto *et al.*, 2018; Ituen *et al.*, 2017; Santos *et al.*, 2020; Santos *et al.*, 2017).

Figure 3: Equivalent electrical circuit model used to adjust carbon steel EIS data in 0.5 mol L⁻¹ HCl in the absence and presence of different concentrations of PRHPPL.



Source: Authors.

The equivalent circuit (Figure 3) presents the charge transfer resistance (R_{ct}) in parallel with the electrical double layer capacitance, taking into account the addition of the constant phase element (CPE_{dl}), both in series with the solution resistance (R_s). The fitting values of the electrochemical parameters were obtained, which are shown in Table 1. It is noteworthy to say that the parameters R_s , R_{ct} , CPE_{dl} and α , from Table 1 were found by adjusting the data referring to the diagrams presented in Figure 2; and the efficiency presented is the average of the efficiency's values founded in the triplicate for each concentration investigated.

Table 1: Electrochemical parameters obtained by the equivalent circuit model of the system of carbon steel in 0.5mol L⁻¹ HCl in the presence of different concentrations of the inhibitor.

Concentration (g.L ⁻¹)	R_s ($\Omega \cdot \text{cm}^2$)	R_{ct} ($\Omega \cdot \text{cm}^2$)	CPE_{dl} ($\text{F} \cdot \text{cm}^2$)	α	$IE \pm SD$ (%)
Blank	6.25	18.41	2.62×10^{-4}	0.87	-
0.44	6.10	155.8	1.11×10^{-4}	0.86	79 ± 7
0.77	6.04	262.5	1.07×10^{-4}	0.86	93 ± 4
1.11	5.76	1033	7.95×10^{-5}	0.87	97 ± 1
1.44	6.29	1632	6.83×10^{-5}	0.89	97.4 ± 0.7
1.77	6.02	2084	5.63×10^{-5}	0.89	98 ± 1

Source: Authors.

The double-layer phase constant element (CPE_{dl}) is a parameter used to replace the pure double-layer capacitor, since the surface of the material under study (carbon steel) presents roughness and heterogeneity which promotes a displacement of the semicircle of the Nyquist diagram (Figure 2.a), presenting a non-ideal capacitor behavior. The impedance of this element is mathematically given by equation 1 (Barreto *et al.*, 2018):

$$Z_{CPE} = Y_0^{-1} (j\omega)^{-\alpha} \quad (1)$$

Where: Y_0 is the value of CPE_{dl} , α is the dispersion factor (varies from 0 to 1) and informs the deviation from the ideal behavior, ω is the angular frequency and j is equal to -1 (Barreto *et al.*, 2018).

In Table 1, it is observed that there is a decrease in the CPE_{dl} value as the inhibitor concentration increases. The highest value found was in the absence of the inhibitor ($2.62 \times 10^{-4} \text{ Fcm}^{-2}$) and the lowest value was obtained at the concentration of 1.77 g L⁻¹ ($5.63 \times 10^{-5} \text{ Fcm}^{-2}$). The values of the dispersion factor (α) presented values between 0.87 and 0.89 proving the need of using a CPE and not a pure capacitor.

The EIS was performed in triplicate for each condition, therefore, the efficiency was found by calculating the average of the efficiencies obtained for each condition. Table 1 shows that the increase in the concentration of the inhibitor promoted

an increase in its efficiency. The highest concentration was the one with the highest efficiency ($98 \pm 1\%$), even for the lowest concentration an efficiency higher than 70% was obtained ($79 \pm 7\%$ at 0.44 gL^{-1}), which is the standard value established by Uhlig (1971) for an inhibitor to be considered minimally efficient. The efficiency from the adjustment to equivalent circuit model was calculated using equation 2 (Santos *et al.*, 2017):

$$IE(\%) = \frac{R_{ct} - R_{ct,0}}{R_{ct}} \quad (2)$$

where: $R_{ct,0}$ is the charge transfer resistance in the absence of inhibitor and R_{ct} represents the charge transfer resistance in the presence of the inhibitor.

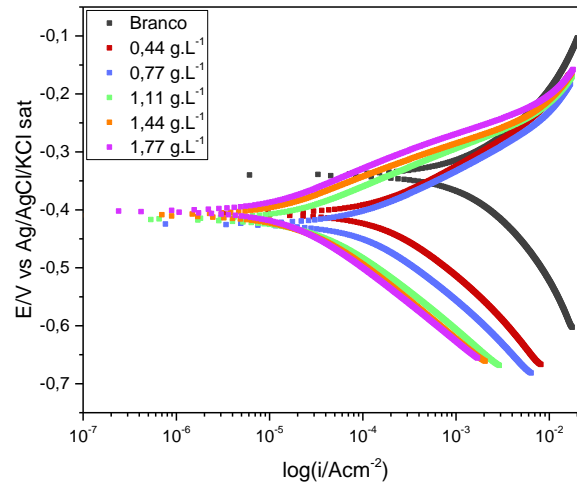
Shalabi and Nazeer (2015) analyzed the methanol extract of fresh parts of Aroeira, cultivated in Egypt, in 0.5 mol.L^{-1} HCl medium; the extract was studied at concentrations ranging from 100 to 900 ppm. The results showed, as well as the results of the present study, that the efficiency increased with the increase in the concentration of the extract, reaching a maximum value of 93 % at 900 ppm and even for the lowest concentration an efficiency higher than 70% was obtained (87 % at 100ppm).

3.1.3 Potentiodynamic polarization curves

The polarization curves obtained for carbon steel in HCl medium at 0.5 mol L^{-1} in the absence and presence of different concentrations of PRHPPL can be seen in Figure 4. The electrochemical parameters, corrosion potential (E_{corr}), the current density (i_{corr}) and the cathodic (β_c) and anodic (β_a) Tafel slopes for the curves shown in Figure 4, can be seen in Table 2. This table also shows the value of the efficiency obtained in all the curves found for each concentration analyzed, since it was performed in triplicate.

From the polarization curves (Figure 4) it is observed, qualitatively, that the presence of the inhibitor from the powder of the hydrodistillation residue of the pink pepper leaf decreased the current density for both the anodic and cathodic curves branches. This decrease in current density is confirmed, quantitatively, by the values shown for the parameter (i_{corr}) in Table 2. The i_{corr} for the blank showed a higher value ($758 \mu\text{A}$) and this value decreased as the inhibitor concentration increased, reaching a lower value at the concentration of 1.77 g L^{-1} ($10.6 \mu\text{A}$).

Figure 4: Tafel curves for carbon steel in the absence and presence of different concentrations of PRHPPL in 0.5mol L⁻¹ HCl medium at room temperature.



Source: Authors.

With the current density obtained, the efficiency of PRHPPL as a corrosion inhibitor was calculated through equation 3 (Santos *et al.*,2020):

$$IE(\%) = \frac{i_{corr}^0 - i_{corr}}{i_{corr}^0} \quad (3)$$

Where: i_{corr}^0 is the current density in the absence of the inhibitor and i_{corr} the current density in the presence of the inhibitor.

Table 2 shows the average values of the efficiency and corresponding standard deviation for the triplicate for each different concentration. The efficiencies values show that increasing the inhibitor concentration increases the protection of carbon steel. The values of Tafel slopes (β_c and β_a) reveal that the corrosion inhibitor studied has a mixed behavior, since its presence is capable of altering the anodic and cathodic currents, promoting the reduction of both (Santos *et al.*,2020). This behavior is common for organic inhibitors. Shalabi and Nazeer (2015) in the evaluation of the extract of different parts of the species *Schinus terebinthifolius* cultivated in Egypt as an inhibitor of corrosion of carbon steel, indicated a mixed performance of the mentioned inhibitor. Carvalho et al (2022) detected mixed behavior in their evaluation of cocoa bean husk powder as an inhibitor of corrosion of carbon steel in acidic medium.

Table 2: Kinetic parameters obtained by extrapolation of Tafel lines for carbon steel in 0.5 mol L⁻¹ in the absence and presence of different concentrations of PRHPPL at room temperature.

Concentration (g.L ⁻¹)	E _{corr} (mV) X Ag/AgCl/KCl Sat	i _{corr} (μA)	$-\beta_c$ (mV/dec)	β_a (mV/dec)	IE \pm SD (%)
Blank	-336	758	155.90	147.44	-
0.44	-427	106	108.83	77.40	78 \pm 7
0.77	-425	65.00	114.24	75.42	94 \pm 3
1.11	-417	17,00	105.02	65.14	97 \pm 1
1.44	-410	11.30	106.18	61.77	97.8 \pm 0.3
1.77	-404	10.60	106.41	66.41	97.8 \pm 1

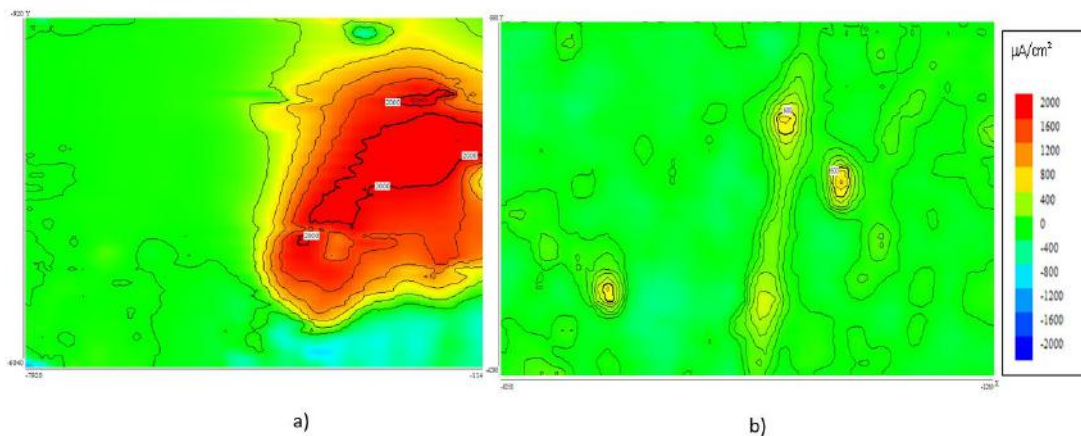
Source: Authors.

3.1.4 Scanning vibrating electrode technique (SVET)

The SVET data were obtained in a solution 0.01 mol L⁻¹ HCl in the absence of the inhibitor and also by adding 1.77 g.L⁻¹ of PRHPPL, the best condition indicated by the EIS technique, in a solution of HCl 0.01 mol.L⁻¹, in the presence of inhibitor. The concentration of the corrosive medium for this technique was less aggressive than the concentration used in the EIS and other tests of the present work (0.5 mol.L⁻¹) to avoid hydrogen bubbles evolution during the test. Figure 5 shows the SVET maps in the absence and presence of the inhibitor after 30 min of immersion.

The analysis of the maps shows the aggressiveness of the medium without the inhibitor (blank), where the presence of regions with anodic ionic currents is observed, evidenced by the yellow and red color. The addition of PRHPPL to the corrosive medium promoted a reduction in the aggressiveness of this medium on the surface of the carbon steel, a fact evidenced by the lower intensity of the anodic and cathodic current, when compared to the blank sample. This reduction in the ionic current density proved that the inhibitor act reducing the corrosive process at metal surface.

Figure 5: SVET ionic current maps for SAE 1008 carbon steel in the absence (a) and presence of PRHPPL (b), after immersion time of 30 min in HCl at 0.01 mol L⁻¹.



Source: Authors.

3.2 Gravimetric tests

The mass loss test was performed using a carbon steel plate prepared as specified in item 2.2. The sample was immersed in the electrolyte of HCl 0.5 mol L⁻¹ for a period of 2 hours, in the absence and presence of different concentrations of PRHPPL. The parameters were obtained: corrosion rate (C_R) (g.cm⁻².h⁻¹), corrosion current density (i_{corr}), degree of steel surface coverage (θ) and the efficiency % of the inhibitor under study. The corrosion rate was calculated using Equation 4; where ΔW is the mass variation of the sample in grams, A is the total area exposed in the solution in cm² and t is the immersion time in seconds (Barreto *et al.*,2017).

$$CR = \frac{\Delta W}{At} \quad (4)$$

Equation 5 was used to calculate the current density, which relates the corrosion rate (C_R) with the Faraday constant (96500 C.mol⁻¹) and the equivalent gram of the electrode used (Eq_{metal}), as the electrode is carbon steel, the value adopted was 27.93 g, corresponding to pure iron (Barreto *et al.*, 2018)

$$i_{corr} = C_R \times \frac{96500}{E_{qmetal}} \quad (5)$$

The efficiency of PRHPPL (η) was obtained by Equation 6, where C_{R0} is the corrosion rate in the absence of the inhibitor and C_R is the corrosion rate in the presence of the inhibitor. With the efficiency values obtained, the degree of coverage of the steel surface was calculated through equation 7 (Santos *et al.*,2020).

$$\eta = \frac{C_{R0} - C_R}{C_{R0}} \times 100 \quad (6) \quad \text{e} \quad \theta = \frac{\eta}{100} \quad (7)$$

The results of the averages of C_R, i_{corr}, θ and η for triplicate for each condition analyzed, are found in Table 3. The analysis of Table 3, allows to infer that the presence of the PRHPPL inhibitor promotes a reduction in the corrosion rate (C_R) and current density (i_{corr}) and with increasing concentration of this inhibitor, this reduction is accentuated. In addition, it appears that there is an increase in the degree of coverage as the concentration of the inhibitor increases, which may be an indication of a possible increase in the adsorption effectiveness of the inhibitor on the steel surface, with the increase in its concentration. The highest concentration (1.77 g L⁻¹) had the best efficiency, reaching a value of 86 %.

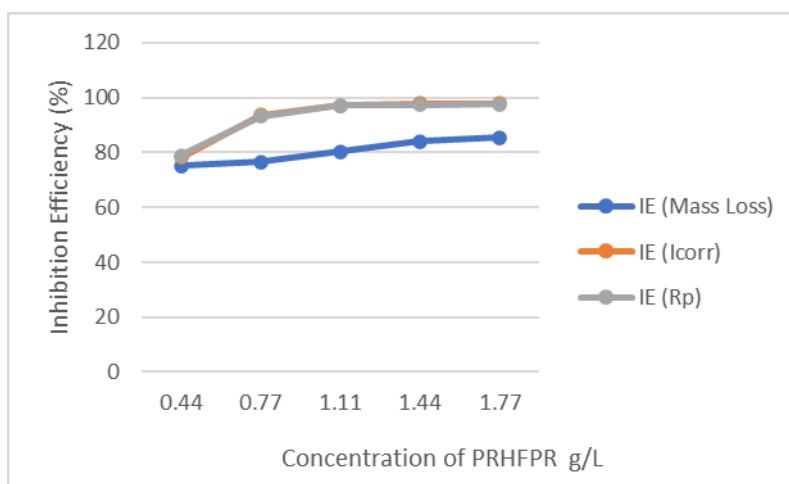
Table 3: Results of the gravimetric test for samples immersed in 0.5mol L⁻¹ HCl medium during 2 hours.

Concentration (g.L ⁻¹)	C _R (g.cm ⁻² .h ⁻¹)	i _{corr} (A.cm ⁻²)	θ	η ±SD (%)
Blank	8.41x 10 ⁻⁴ ±3.73 x 10 ⁻⁴	8.08 x 10 ⁻⁴	-	-
0.44g.L ⁻¹	2.08 x 10 ⁻⁴ ±3.35 x 10 ⁻⁵	2.00 x 10 ⁻⁴	0.753	75 ± 4
0.77g.L ⁻¹	1.97 x 10 ⁻⁴ ±2.74 x 10 ⁻⁵	1.89 x 10 ⁻⁴	0.765	77 ± 3
1.11 g.L ⁻¹	1.65 x 10 ⁻⁴ ±4.86 x 10 ⁻⁵	1.59 x 10 ⁻⁴	0.803	80 ± 6
1.44g.L ⁻¹	1.34 x 10 ⁻⁴ ±1.54 x 10 ⁻⁵	1.28 x 10 ⁻⁴	0.841	84 ± 2
1.77g.L ⁻¹	1.22 x10 ⁻⁴ ±2.89 x 10 ⁻⁵	1.17 x 10 ⁻⁴	0.855	86 ± 3

Source: Authors.

Figure 6 shows a graph showing the relationship between the efficiency of the PRHFPR inhibitor with the different concentrations studied for the different methods (Icorr, Rp and mass loss). The analysis of the graph allows us to infer that the efficiency obtained by the Icorr and Rp methods presented very close and high values. The mass loss test presented the lowest values, however, all efficiency values are above 70%, a value indicated by the classical literature as demonstrating the good performance of an inhibitor (Uhlig,1971). It can be seen in Table 3 that even the addition of the lowest concentration of the inhibitor (0.44 g L^{-1}) promotes good efficiency in protecting the steel surface. This result was also supported by the techniques used above.

Figure 6: Concentration of PRHFPR X Inhibition Efficiency in $\text{HCl } 0.5\text{mol.L}^{-1}$.



Source: Authors.

3.3 Adsorption Isotherms

In order to understand the interaction that occurs between the carbon steel surface and the PRHPPL inhibiting molecules, a theoretical mathematical treatment of the adsorption process by isotherms was carried out. Different isotherm models were tested using the different concentrations of the inhibitor and the degree of coverage of the carbon steel surface, seen in Table 4.

The tested isotherms were Langmuir, Freundlich, Temkin, Flory-Huggins and Frumkin using their respective equations, observed in Table 4. The K parameter is the equilibrium constant of the inhibitor adsorption process, C is the concentration of the inhibitor; θ is the degree of surface coverage; K_f is the Freundlich constant and n indicates whether the process is favorable or not, when n is in the range from 1 to 10. The x represents the number of water molecules replaced by the inhibitor molecules and g is the constant that indicates the degree of interaction side between the adsorbed molecules (Fateh *et al.*, 2017).

Table 4 shows the adsorption parameters obtained and their respective correlation coefficients of the straight lines (R^2). The analysis of Table 4 shows that the Langmuir isotherm presented the highest correlation coefficient (0.9980) while the Frumkin isotherm presented the worst fit (0.6536). As a result, the molecules present in the PRHPPL responsible for inhibiting the corrosion of carbon steel adsorb better following the Langmuir isotherm. The adsorption of inhibitor molecules, according to the Langmuir isotherm, occurs in a monolayer on the metallic surface; and each active site presented in this surface is occupied by only one inhibitor molecule. This fact may be linked to the better linearity achieved by this isotherm and indicated by the slope closer to 1 that it reached (Hussin *et al.*, 2016).

Table 4: Parameters obtained for different adsorption isotherms.

Isortherms	Equations	R ²	Line Equation
Langmuir (C/θ) versus C)	$\frac{C}{\theta} = \frac{1}{K} + C$	0.9980	y = 1.1044x + 0.1297
Freundlich(log θ versus logC)	$\log \theta = \log K_f + \frac{1}{n} \log C$	0.9168	y = 0.0975x - 0.0953
Temkin (θ versus logC)	$\theta = \frac{2.303}{a} \log K + \frac{2.303}{a} \log C$	0.9116	y = 5.0747x - 4.0807
Flory-Huggins (log(θ/C) versus log(1-θ))	$\log \frac{\theta}{C} = \log K + x \log(1 - \theta)$	0,8675	y = 1.977x + 1.3232
Frumkin (log(θ/(1-θ).C) versus θ)	$\log \frac{\theta}{(1 - \theta).C} = \log K + g\theta$	0.6536	y = -2277x + 2,4532

Source: Carvalho et al.,2022; Authors.

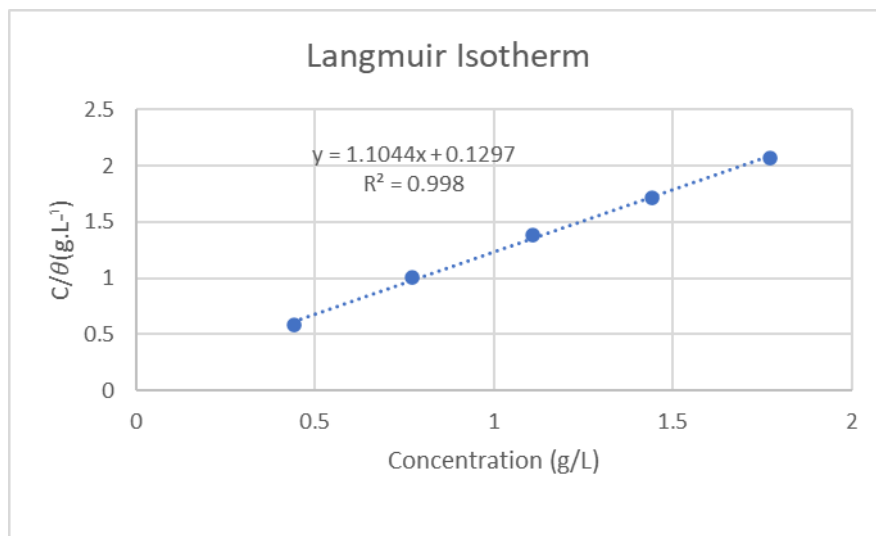
Figure 7 shows the graph of the Langmuir isotherm with its equation of the straight line, from this equation it is possible to find the adsorption constant (k). The value of k is 7.710 L g⁻¹ and with this value, considering the temperature of 298K and using Equation 8, the Gibbs free energy of adsorption (ΔG°_{ads}) was obtained, whose value is - 22.177 kJ.mol⁻¹.

$$\Delta G_{ads}^0 = -RT \ln (C_{H_2O} \cdot k) \quad (8)$$

Where: T is the absolute temperature, R is the universal gas constant (whose value is 8.3147 J.mol⁻¹K⁻¹), C_{H₂O} is the concentration of water and its value is 55.5 mol L⁻¹ (1000 g.L⁻¹).

The negative value (- 22.177 kJ. mol⁻¹) of the Gibbs adsorption free energy allows to say that the inhibitor molecules adsorb spontaneously on the carbon steel surface. Furthermore, this value indicates that the adsorption of the molecules responsible for reducing the corrosion of carbon steel occurs by physical adsorption, since the value of ΔG°_{ads} is around -20 kJ mol⁻¹ (Hussin *et al.*,2016). The Langmuir isotherm was also the best fit in the study by Shalabi and Nazeer (2015), the authors used extracts from different parts in nature of Aroeira. The value for the free energy of Gibbs adsorption found by the authors was 20.72 kJ mol⁻¹, which is close to the one obtained in this study.

Figure 7: Langmuir's isotherm for SAE 1008 carbon steel containing different concentrations of PRHPPL in 0.5 mol L⁻¹ HCl solution.



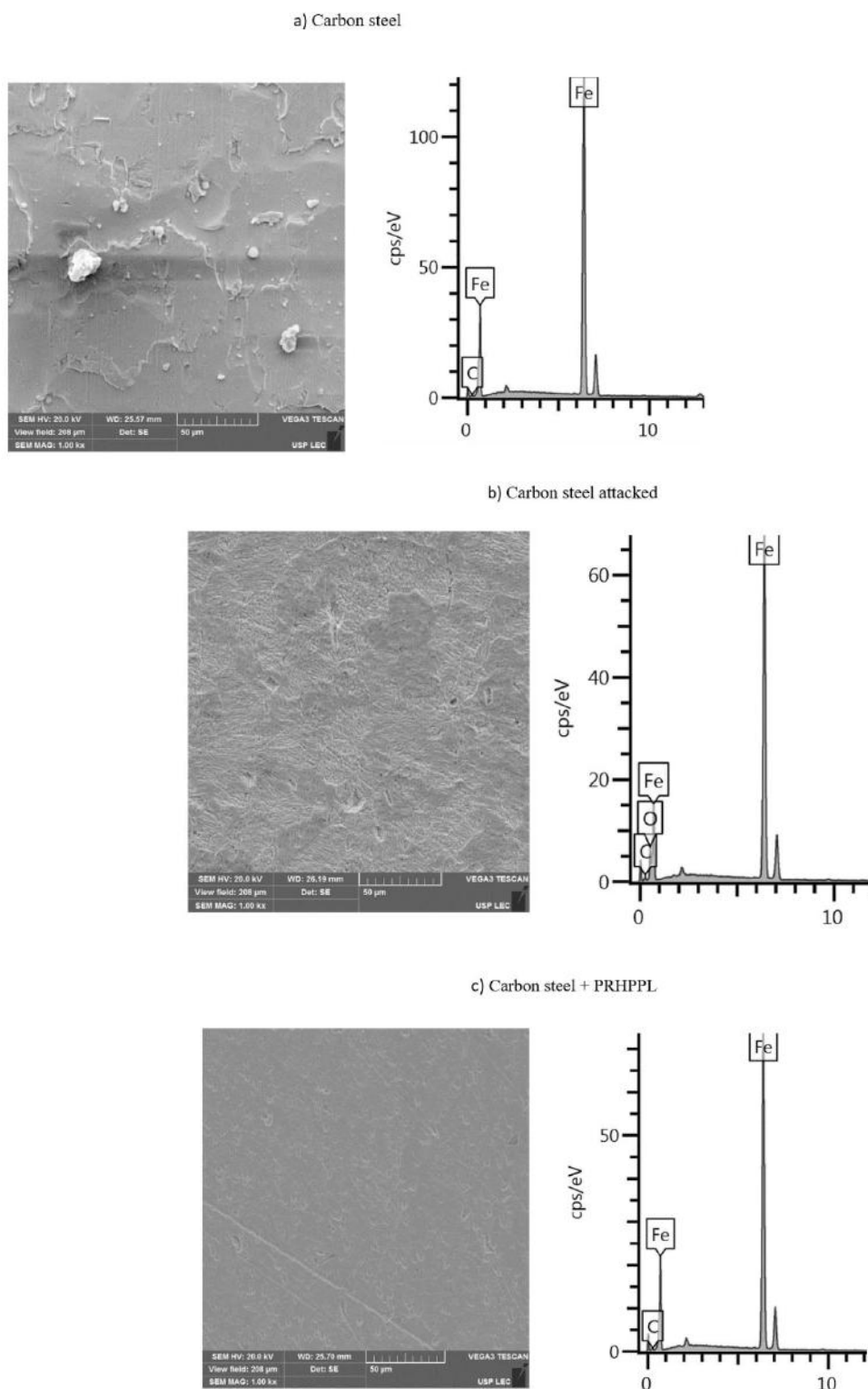
Source: Authors.

3.4 Carbon Steel Surface Characterization

To prove the action of the PRHPPL inhibitor on the carbon steel surface, scanning electron microscopy (SEM) and energy dispersive spectroscopy (EDS) tests were performed. The SEM and EDS images of the 1008 carbon steel sample were obtained before immersion (Figure 8.a) and, with immersion in a 0.5 mol L⁻¹ HCl solution in the absence (Figure 8.b) and after immersion in presence of the PRHPPL (Figure 8.c).

It is observed that before immersion (Figure 8 a) the carbon steel sample, has a roughness profile, with some sandpaper abrasive residue in its surface. In the EDS elemental analysis, it is possible to see that no significant amount of oxygen was founded, concluding that corrosion process did not take place. It is noticed that after immersion in the corrosive medium (Figure 8.b) there is the presence of corrosion products throughout the steel sample (generalized corrosion), confirmed by the significant value of oxygen and iron elements in the EDS analysis. In the steel sample after immersion in the presence of the inhibitor (Figure 8.c), a reduction in the corrosion product is observed when compared to the image in the absence of the inhibitor (Figure 8.b), evidencing that there is adsorption of the inhibitor on the surface of the carbon steel, increasing the corrosion resistance of steel in the corrosive environment in the presence of PRHPPL. This result can be emphasized by the EDS analysis, showing just the peak related to the iron and carbon elements.

Figure 8: SEM images and identification of the EDS chemical elements of the sample before immersion (a), after immersion for 2 h in HCl solution at 0.5 mol L^{-1} (b) and after immersion for 2 h in the presence of the inhibitor at concentration of 1.77 g.L^{-1} (c).



Source: Authors.

4. Conclusion

In view of the results obtained, it can be concluded that the green corrosion inhibitor from the solid residue powder of the hydrodistillation of the essential oil of the pink pepper leaf, has the potential to be used to control the corrosion of the SAE 1008 carbon steel alloy. Electrochemical and gravimetric tests showed that the inhibition efficiency increases when larger amounts of the powder were added to the aggressive solution. The concentration of 1.77 g L^{-1} showed efficiency of 98 % in electrochemical tests and 86 % in gravimetric tests. The lowest concentration of the inhibitor (0.44 g L^{-1}) also showed good efficiency 79 % (electrochemical) and 75 % (gravimetric).

The SVET measurements show that in the presence of the PRHPPL inhibitor both the anodic and cathodic ionic currents were reduced. The SEM images show a small reduction in corrosion points in the test with the presence of the inhibitor, proving the presence of molecules on the metal surface. The adsorption of the inhibitor on the carbon steel surface in HCl solution follows the Langmuir isotherm.

It can also be inferred that this inhibitor, in addition to being environmentally friend will help to protect equipment, reducing the cost of corrosion, in addition to adding more value to a plant that is widely cultivated in Brazil and also to the solid residue from the production of essential oils that is little used by industries.

In this research, it was evaluated how to protect carbon steel in an acid medium (HCl). For this medium and substrate, the corrosion inhibitor from the hydrodistillation residue of aroeira leaf proved to be effective. However, corrosion affects different materials and is caused by different atmospheres. As a result, future research can evaluate this same residue as a corrosion inhibitor for other materials, as well as in other corrosive environments.

Acknowledgments

The authors would like to acknowledge to CNPq scholarships – Brazil [National Council for Scientific and Technological Development (grant number: 140187/2017-0)], (Process number: 428512/2018-6 and grant number: 310504/2020-1) and to PROPP/UESC (Pro-Rectorate of Research and Post-Graduation at State University of Santa Cruz) for the financial support; to Usiminas S.A. by the AISI 1008 carbon steel; to Klintex Industrial Resources by the alkaline degreaser to the Environmental and Materials Laboratory and the State University of Santa Cruz (LAMMA/UESC, BA, BR) by the support inputs, and equipment that made this work possible.

References

- Anupama, K. K., Ramya, K., & Joseph, A. (2017). Electrochemical measurements and theoretical calculations on the inhibitive interaction of *Plectranthus amboinicus* leaf extract with mild steel in hydrochloric acid. *Measurement*, 95, 297-305.
- Al Hasan, N. H. J., Alaradi, H. J., Al Mansor, Z. A. K., & Al Shadood, A. H. J. (2019). The dual effect of stem extract of Brahmi (*Bacopamonnieri*) and Henna as a green corrosion inhibitor for low carbon steel in 0.5 M NaOH solution. *Case Studies in Construction Materials*, 11, e00300.
- Baranauskienė, R., Bendžiuvienė, V., Ragažinskienė, O., & Venskutonis, P. R. (2019). Essential oil composition of five *Nepeta* species cultivated in Lithuania and evaluation of their bioactivities, toxicity and antioxidant potential of hydrodistillation residues. *Food and Chemical Toxicology*, 129, 269-280.
- Barreto, L. S., Tokumoto, M. S., Guedes, I. C., Melo, H. G. D., Amado, F. D. R., & Capelossi, V. R. (2017). Evaluation of the anticorrosion performance of peel garlic extract as corrosion inhibitor for ASTM 1020 carbon steel in acidic solution. *Matéria (Rio de Janeiro)*, 22.
- Barreto, L. S., Tokumoto, M. S., Guedes, I. C., Melo, H. G. D., Amado, F., & Capelossi, V. R. (2018). Study and Assessment of the Efficiency of the Cocoa Bark Extracted from the *Theobroma Cacao* as an Inhibitor of the Corrosion of Carbon Steel in Substitution of Benzotriazole. *Materials Research*, 21.
- Carvalho, M. C. F. D., Almeida, N. M. S. D., Silva, I. M. F. C. R., Cotting, F., Aoki, I. V., & Capelossi, V. R. (2022). Electrochemical and Economic Evaluation of the Cocoa Bean Shell as a Corrosion Inhibitor in Acidic Medium. *Materials Research*, 25.
- Divya, P., Subhashini, S., Prithiba, A., & Rajalakshmi, R. (2019). *Tithonia diversifolia* flower extract as green corrosion inhibitor for mild steel in acid medium. *Materials Today: Proceedings*, 18, 1581-1591.
- Elyemni, M., Louaste, B., Nechad, I., Elkamli, T., Bouia, A., Taleb, M., & Eloutassi, N. (2019). Extraction of essential oils of *Rosmarinus officinalis* L. by two different methods: Hydrodistillation and microwave assisted hydrodistillation. *The Scientific World Journal*, 2019.

- Fateh, A., Aliofkhazraei, M., & Rezvanian, A. R. (2020). Review of corrosive environments for copper and its corrosion inhibitors. *Arabian journal of Chemistry*, 13(1), 481-544.
- Hussin, M. H., Rahim, A. A., Ibrahim, M. N. M., & Brosse, N. (2016). The capability of ultrafiltrated alkaline and organosolv oil palm (*Elaeis guineensis*) fronds lignin as green corrosion inhibitor for mild steel in 0.5 M HCl solution. *Measurement*, 78, 90-103.
- Ituen, E., Akaranta, O., James, A., & Sun, S. (2017). Green and sustainable local biomaterials for oilfield chemicals: Griffonia simplicifolia extract as steel corrosion inhibitor in hydrochloric acid. *Sustainable materials and technologies*, 11, 12-18.
- Loto, R. T., Leramo, R., & Oyeade, B. (2018). Synergistic Combination Effect of *Salvia officinalis* and *Lavandula officinalis* on the Corrosion Inhibition of Low-Carbon Steel in the Presence of SO₄²⁻-and Cl⁻-Containing Aqueous Environment. *Journal of Failure Analysis and Prevention*, 18(6), 1429-1438.
- Mahomoodally, F., Aumeeruddy-Elalfi, Z., Venugopala, K. N., & Hosenally, M. (2019). Antiglycation, comparative antioxidant potential, phenolic content and yield variation of essential oils from 19 exotic and endemic medicinal plants. *Saudi journal of biological sciences*, 26(7), 1779-1788.
- Ogunleye, O. O., Arinkoola, A. O., Eletta, O. A., Agbede, O. O., Osho, Y. A., Morakinyo, A. F., & Hamed, J. O. (2020). Green corrosion inhibition and adsorption characteristics of *Luffa cylindrica* leaf extract on mild steel in hydrochloric acid environment. *Heliyon*, 6(1), e03205.
- Palanisamy, S. P., Maheswaran, G., Kamal, C., & Venkatesh, G. (2016). *Prosopis juliflora*—A green corrosion inhibitor for reinforced steel in concrete. *Research on Chemical Intermediates*, 42(12), 7823-7840.
- Saeed, M. T., Saleem, M., Niyazi, A. H., Al-Shamrani, F. A., Jazzar, N. A., & Ali, M. (2020). Carrot (*Daucus carota* L.) peels extract as an herbal corrosion inhibitor for mild steel in 1M HCl solution. *Modern Applied Science*, 14(2), 97-112.
- Shalabi, K., & Nazeer, A. A. (2015). Adsorption and inhibitive effect of *Schinus terebinthifolius* extract as a green corrosion inhibitor for carbon steel in acidic solution. *Protection of Metals and Physical Chemistry of Surfaces*, 51(5), 908-917.
- Sanaei, Z., Ramezanzadeh, M., Bahlakeh, G., & Ramezanzadeh, B. (2019). Use of *Rosa canina* fruit extract as a green corrosion inhibitor for mild steel in 1 M HCl solution: A complementary experimental, molecular dynamics and quantum mechanics investigation. *Journal of industrial and engineering chemistry*, 69, 18-31.
- Santana, J. S., Sartorelli, P., Guadagnin, R. C., Matsuo, A. L., Figueiredo, C. R., Soares, M. G., & Lago, J. H. G. (2012). Essential oils from *Schinus terebinthifolius* leaves—chemical composition and in vitro cytotoxicity evaluation. *Pharmaceutical Biology*, 50(10), 1248-1253.
- Santos, A. D. M., Almeida, T. F. D., Cotting, F., Aoki, I. V., Melo, H. G. D., & Capelossi, V. R. (2017). Evaluation of castor bark powder as a corrosion inhibitor for carbon steel in acidic media. *Materials Research*, 20, 492-505.
- Santos, A. M., Aquino, I. P., Cotting, F., Aoki, I. V., De Melo, H. G., & Capelossi, V. R. (2021). Evaluation of palm kernel cake powder (*Elaeis guineensis* Jacq.) as corrosion inhibitor for carbon steel in acidic media. *Metals and Materials International*, 27(6), 1519-1530.
- Speight, J. G. (2014). *Oil and gas corrosion prevention: From surface facilities to refineries*. Gulf Professional Publishing.
- Tolulope Loto, R., & Olowoyo, O. (2018). Corrosion inhibition properties of the combined admixture of essential oil extracts on mild steel in the presence of SO₄²⁻ anions. *South African Journal of Chemical Engineering*, 26(1), 35-41.
- Uhlig, H. H. (1971) Corrosion and corrosion control: An introduction to corrosion science and engineering. (2a. ed.) John Wiley: New York.
- Uliana, M. P., Fronza, M., da Silva, A. G., Vargas, T. S., de Andrade, T. U., & Scherer, R. (2016). Composition and biological activity of Brazilian rose pepper (*Schinus terebinthifolius* Raddi) leaves. *Industrial Crops and Products*, 83, 235-240.
- Umoren, S. A., Solomon, M. M., Obot, I. B., & Suleiman, R. K. (2019). A critical review on the recent studies on plant biomaterials as corrosion inhibitors for industrial metals. *Journal of Industrial and Engineering Chemistry*, 76, 91-115.
- Velčković, D. T., Milenović, D. M., Ristić, M. S., & Veljković, V. B. (2008). Ultrasonic extraction of waste solid residues from the *Salvia* sp. essential oil hydrodistillation. *Biochemical Engineering Journal*, 42(1), 97-104.
- Zaher, A., Chaoui, A., Salghi, R., Boukhraz, A., Bourkhiss, B., & Ouhssine, M. (2020). Inhibition of mild steel corrosion in 1M hydrochloric medium by the methanolic extract of *Ammi visnaga* L. Lam seeds. *International Journal of Corrosion*, 2020.